Contents lists available at ScienceDirect

Chemical Engineering Research and Design

journal homepage: www.elsevier.com/locate/cherd

Can metal organic frameworks outperform adsorptive removal of harmful phenolic compound 2-chlorophenol by activated carbon?

Luqman Hakim Mohd Azmi[a,b,c], *Daryl Williams*[c], *Bradley P. Ladewig*[a,d,*]

[a] *Barrer Centre, Department of Chemical Engineering, Imperial College London, South Kensington Campus, SW7 2AZ, London, United Kingdom*

[b] *Grantham Institute – Climate Change and the Environment, Imperial College London, South Kensington Campus, SW7 2AZ, London, United Kingdom*

[c] *Surfaces and Particle Engineering Laboratory, Department of Chemical Engineering, Imperial College London, South Kensington Campus, SW7 2AZ, London, United Kingdom*

[d] *Institute for Micro Process Engineering (IMVT), Karlsruhe Institute of Technology, Hermann-von-Helmholtz-Platz 1, 76344 Eggenstein-Leopoldshafen, Germany*

ARTICLE INFO

Article history:
Received 19 November 2019
Received in revised form 9 March 2020
Accepted 11 March 2020
Available online 1 April 2020

Keywords:
2-Chlorophenol
Activated carbon
Liquid adsorption
Metal organic frameworks
Organic pollutant removal

ABSTRACT

Removal of persistent organic compounds from aqueous solutions is generally achieved using adsorbent like activated carbon (AC) but it suffers from limited adsorption capacity due to low surface area. This paper describes a pioneering work on the adsorption of an organic pollutant, 2-chlorophenol (2-CP) by two MOFs with high surface area and water stability; MIL-101 and its amino-derivative, MIL-101-NH_2. Although MOFs have higher surface area than AC, the latter was proven better having the highest equilibrium 2-CP uptake (345 mg g^{-1}), followed by MIL-101 (121 mg g^{-1}) and MIL-101-NH_2 (84 mg g^{-1}). Used MIL-101 could be easily regenerated multiple times by washing with ethanol and even showed improved adsorption capacity after each washing cycle. These results can open the doors to meticulous adsorbent selection for treating 2-CP-contaminated water.

© 2020 Institution of Chemical Engineers. Published by Elsevier B.V. All rights reserved.

1. Introduction

The need for clean water source is central to everyone's lives. However, continuous growth of global population causes water demand to increase at an alarming rate of 1% per year (United Nations World Water Assessment Programme, 2018). Adding into that conflict is the significant change in our consumption patterns; driving the need for more product variety to fulfil our daily needs. As a result, numerous chemicals are produced and dispensed for applications in medicine, industry, agriculture and common household conveniences (Kolpin et al., 2002). Although humans benefit from the unprecedented production, the widespread industrial discharges to the environment contain a myriad of synthetic chemicals used in the manufacturing of solvents, plasticizers and pesticides (Olaniran and Igbinosa, 2011; The United Kingdom Parliamentary Office of Science and Technology, 2018). Some substances, particularly aromatic compounds like chloro-(CP), nitro-(NP) and other substituted phenols have been found to be persistent and bio-refractory in the aqueous environment and in waste water treatment plants (Shang et al., 2006). To date, there is a total of 19 existing chlorinated phenols (World Health Organization, 2003) but in this work, 2-chlorophenol (2-CP) will be evaluated as a model pollutant given its potential carcinogenicity and toxicity risks towards wildlife and human health. 2-CP is a potent endocrine disrupting agent (Sharma et al., 2013). It is classified as one of the priority pollutants by the United

* *Corresponding author at*: Barrer Centre, Department of Chemical Engineering, Imperial College London, South Kensington Campus, SW7 2AZ, London, United Kingdom.
E-mail address: bradley.ladewig@kit.edu (B.P. Ladewig).
https://doi.org/10.1016/j.cherd.2020.03.017
0263-8762/© 2020 Institution of Chemical Engineers. Published by Elsevier B.V. All rights reserved.

States Environmental Protection Agency (United States Environmental Protection Agency, 2014) and also listed in the European Parliament Decision No. 2455/2001/EC (European Communities, 2001) highlighting the stringent need of monitoring and regulation required for this chemical.

Moreover, CPs are suspected precursors of very toxic compounds like polychlorodibenzo-p-dioxins (PCDDs), polychlorodibenzofurans (PCDFs) and polychlorophenoxyphenols (PCPPs). They are part of the 2001 Stockholm Convention's persistent organic pollutants (POPs) watch list. The ratified agreement requires involving parties to take cooperative action in reducing or totally eliminate any form of production or discharge of the compounds as they can potentially deteriorate human health and the environment (Luo et al., 2006; Stockholm Convention Secretariat United Nations Environment, 2017). CPs are known for having strong organoleptic effects with low taste thresholds (0.1 ppb) when present in water. Principal sources of 2-CP stem from industrial chlorination during disinfection, as by-products from the reaction of hypochlorite with phenolic acids, from biocides or the degradation result of phenoxy-containing herbicides (Aksu and Yener, 2001; World Health Organization, 2003). Their concentrations vary depending on the kind of reservoirs (lakes, rivers, oceans) but typically exist in trace parts per billion, ppb (ng L^{-1}) range (Czaplicka, 2004).

Latest reports on treatment of 2-CP include using biological methods (Liang et al., 2018; Martínez-Jardines et al., 2018; Sun et al., 2018), adsorption (Chuang et al., 2008; Gan et al., 2018; Smolin, 2018), photocatalytic degradation (Dobaradaran et al., 2018; Zhang et al., 2018) and advanced oxidation processes (Li et al., 2019). Among all technologies, adsorption has a number of key advantages including easy to handle, high removal efficiency for pollutants at low concentration, no generation of toxic intermediates or secondary products and its comparatively low cost to other treatment processes (Hadjltaief et al., 2018; Jang et al., 2018). Furthermore, because aromatic compounds possess low biodegradability in water (Aktaş and Çeçen, 2007), removal of toxic organics is limited if subjected to biological treatment method *per se* (Vashi et al., 2018). Therefore, a combined system involving pre-treatment of the wastewater with biological method followed by adsorption will yield promising removal result.

Activated carbon (AC) is the traditionally used adsorbent in industries to remove these contaminants (Moura et al., 2018) but recently developed porous materials, known as metal organic frameworks (MOFs) is taking centre stage surpassing AC performance in separation processes (Hasan et al., 2013, 2012; Hasan and Jhung, 2015; Khan et al., 2015; Van de Voorde et al., 2014). MOFs are attractive with their superior properties like high surface area, good thermal stability and the versatility of in-pore or outer-surface modification to suit diverse form of applications (Gu et al., 2012; Seo et al., 2016). Apart from that, MOFs can be reused using a very simple solvent exchange technique (Han and Lah, 2015) in comparison to incineration or high-temperature activation (up to 800 °C) for spent AC. The costly thermal regeneration process sometimes yields little benefit over the cost of buying fresh AC (Sühnholz et al., 2018). To our knowledge, no literature has attempted to explore the possibility of using MOFs to remove harmful organic pollutant 2-CP from dilute aqueous solutions. On that basis, in this work, the uptake of 2-CP will be tested using two MOFs with high surface area and good water stability, MIL-101 along with its amine-functionalized analogue, MIL-101-NH_2 against a commercial AC as the benchmark.

2. Material and methods

2.1. Materials and chemicals

All chemicals used in this work were purchased from commercial suppliers and used without further purification. Chromium (III) nitrate nonahydrate ($Cr(NO_3)_3.9H_2O$, 98.5%) was obtained from Alfa Aesar. Terephthalic acid (H_2BDC, 98%) and chromium (III) chloride hexahydrate ($CrCl_3.6H_2O$, 96%) were purchased from Sigma-Aldrich. Anhydrous tin (II) chloride ($SnCl_2$, 98%) and 2-chlorophenol (C_6H_5ClO, 98%) were purchased from Acros Organics. 2-nitroterephthalic acid (NO_2-BDC, 95%) was purchased from Fluorochem. Solvents including ethanol (EtOH, 100%), N, N-Dimethylformamide (DMF, 99.9%) glacial acetic acid (AcOH, 100%), hydrochloric acid (HCl, 37%) and sodium hydroxide (NaOH, 50%) were all procured from VWR Chemicals. Working solutions were diluted accordingly with ultrapure water obtained from PureLab Chorus ELGA. Granular AC F400, supplied by Chemviron Carbon was prepared from high grade bituminous coal and steam activated (Chemviron Carbon, 2013; Morlay et al., 2005).

2.2. Hydrofluoric acid free synthesis of MIL-101 and MIL-101-NH_2

Synthesis of MIL-101 was adapted from a previously reported method (Karikkethu Prabhakaran and Deschamps, 2015). $Cr(NO_3)_3.9H_2O$ (2 g), H_2BDC (0.83 g) and AcOH (0.29 mL) and 25 mL of ultrapure water were mixed in a 50 mL Teflon-lined bomb. The mixture was later sealed and heated in an oven at 220 °C for 8 h. When it cooled down to room temperature, the resultant fine, green crystals were thoroughly washed with DMF (20 mL × 3) and EtOH (20 mL × 3). Washing with each solvent was repeated thrice to clear unreacted H_2BDC from the product. The suspensions were centrifuged and then evacuated under vacuum condition at 120 °C for 12 h to obtain dehydrated MIL-101.

Amino-functionalized MIL-101-NH_2 was synthesized according to an already reported method (Bernt et al., 2011). $CrCl_3.6H_2O$ (0.27 g) and NO_2-BDC (0.21 g) were suspended with 5 mL ultrapure water in a 25 mL Teflon-lined bomb. The bomb was left in a preheated oven for 96 h at 180 °C. The resultant green solid was centrifuged, washed and dried according to the aforementioned steps. The final product was designated as MIL-101-NO_2 which serves as an intermediate to obtain MIL-101-NH_2. Continuing from the previous synthesis, 0.1 g of MIL-101-NO_2, 3.3 g of $SnCl_2.2H_2O$ and 20 mL EtOH were mixed, heated and continuously stirred in an oil bath kept at 70 °C for 6 h. After it cooled down, it was centrifuged, washed with concentrated HCl (20 mL × 1), water (20 mL × 3) and EtOH (20 mL × 1) before finally dried under the same condition mentioned before.

2.3. Characterization

Powder X-Ray Diffraction (PXRD) spectra was collected using X'Pert PRO PANalytical equipment with Cu K α radiation (20 mA, 40 kV) within a scattering angle range, 2θ (°) between 5° and 30°. Simulated PXRD spectra for MIL-101 was obtained from Mercury version 3.9 software suite with CCDC code of OCUNAC. N_2 adsorption and desorption isotherms were conducted with surface area analyser Micromeritics 3Flex at liquid nitrogen temperature (77 K) using a partial pressure (p/p_o) range from 0 to 0.99. The specific surface area was calculated using Brunauer-Emmett-Teller (BET) method. Fourier Transform Infrared (FTIR) spectra was analysed using Perkin Elmer Spectrum 100 FT-IR Spectrometer. Ultraviolet–visible (UV–vis) analysis was measured with Perkin Elmer Lambda 35 UV/VIS spectrometer. The thermal stability of all adsorbents was investigated using thermogravimetric analysis (TGA) instrument Netzsch STA 449 F5 Jupiter in N_2 atmosphere. Temperature was ramped from 20 °C to 1000 °C with a heating rate of 20 °C min^{-1}. The zeta potential and particle size distribution of the adsorbents were analysed by BrookHaven

Instruments ZETA PALS in 500 ppm 2-CP solution with 0.01 M NaCl as electrolyte. The morphology of the MOFs were studied using Scanning Electron Microscopy (SEM). SEM images were collected with a high-resolution Schottky field emission gun scanning electron microscope (Zeiss Auriga Cross Beam) operating at 5 kV. Samples were first coated with chromium (15 nm thick) to permit conductivity. The elemental analysis (CHNS) were conducted with a CHNS analyser (Vario MICRO CUBE, Elementar). The instrument uses Helium as a carrier and flushing gas and the combustion is carried out by pulse injection of oxygen. KRUSS Drop Shape Analyzer was used to measure water contact angle of MIL-101 at ambient temperature. To prepare the sample, about 150 mg of MIL-101 was pressed into a pellet form. Prior to any measurements, samples were degassed at 120 °C under vacuum for 12 h to clear the pores from any solvent molecules.

2.4. Batch adsorption

Pollutant removal experiment was referred from a reported method (Hasan et al., 2013) with some modifications. A stock 2-CP solution (1000 ppm) was prepared and diluted successively with ultrapure water to obtain desired concentrations. A calibration curve was generated from the UV–vis spectra of standard 2-CP solutions (5–50 ppm) using the maxima absorbance wavelength (=274 nm) (Fig. S1 in SI). 5 mL 2-CP solution of different concentrations and 5 mg of each adsorbent (AC, MIL-101, MIL-101-NH2) were added respectively into scintillation vials containing magnetic stir bars. The solutions were continuously stirred and left to reach equilibrium for 24 h under ambient temperature. After the designated period, the mixtures were filtered with 0.22 μm syringe filters. The filtrate was then diluted (0.5 mL aliquot: 10 mL ultrapure water). Residual 2-CP concentration for the samples was characterized using UV–vis spectroscopy. All experiments were carried out in triplicates. The amount of 2-CP adsorbed was calculated using Eq. (1):

$$q_t = (C_0 - C_t)\frac{V}{m} \quad (1)$$

where Co and Ct (mg.L−1) are initial and final concentrations of the solution accordingly. V (L) and m (g) represent solution volume and mass of adsorbent respectively.

2.5. Kinetic study

For the purpose of kinetic study, a 2-CP stock solution of 500 ppm was used. Only AC and MIL-101 were tested. 5 mg of dried adsorbents were added into scintillation vials and then topped up with 10 mL of the pollutant stock solution. The contents were stirred and after specific time intervals, 2 mL aliquot of the suspension was extracted using syringe and immediately filtered with 0.22 μm syringe filters. The filtrate was further diluted (1 mL aliquot: 10 mL ultrapure water) to prepare for UV–vis spectroscopy measurements. Adsorption capacity for each particular amount of time was calculated using Eq. (1).

2.6. pH influence

Adsorption experiment was performed at different pH values (1–13) using 500 ppm 2-CP as the stock solution. The adsorption experimental set up and calculation for adsorption capacity can be referred to the template mentioned in Section 2.4.

3. Results and discussion

3.1. PXRD

MIL-101 is commonly synthesized based on hydrothermal method using hydrofluoric (HF) acid as additive. As HF is a very corrosive acid (pK_a = 3.45) (Burgher et al., 2011), the associated injuries from misuse can be horrendous. To reduce potential hazards, acetic acid has been regularly used as a substitute (Rallapalli et al., 2016; Sonnauer et al., 2009; Zhao et al., 2017, 2015) likewise in this study for a successful synthesis of MIL-101. It can be confirmed from the PXRD spectra of the prepared MIL-101 with the simulated pattern (Fig. S2 in SI). Similar resemblance was also observed for MIL-101-NH_2 indicating retained materials crystallinity after modification. Meanwhile, for AC, the only peak appearing at 27° indicates the presence of quartz or SiO_2 (Ismail et al., 2015). The aqueous stability of MIL-101 was also probed by immersing the MOF for 3 days in pH 1 and pH 11 solutions (Fig. S3 in SI).

3.2. Surface area analysis

With reference to Table 1 and (Fig S4 in SI), in the order of decreasing surface area, MIL-101 has the highest BET surface area (2710 $m^2\ g^{-1}$) followed by MIL-101-NH_2 (1983 $m^2\ g^{-1}$) and lastly AC (1179 $m^2\ g^{-1}$). Post-immersion surface area analysis shows outstanding MOF resistance towards acidic environment given negligible surface area reduction. Oppositely, a highly alkaline condition is detrimental to the framework as it started to lose some of its porosity. It is presumed that MIL-101 is stable in acidic condition because acetic acid was used as an additive. However, when the alkalinity level increases, the Cr^{3+} metal sites are prone to degradation, hence, slightly collapsing the framework. Complete N_2 adsorption and desorption isotherms can be found in Fig. S5 in SI.

3.3. FTIR

A comparison between Fourier Transform Infra-Red (FTIR) spectra of pristine MIL-101 and saturated MIL-101 is shown in Fig. S6 in SI. Based on the spectra, none of the peaks on the pristine MOF shifted, meaning there is no new bond formation. Our initial assumption is that adsorption of 2-CP takes place via physical sorption. Using the equilibrium maximum adsorption capacity of MIL-101 (121 mg g^{-1}), it is understood only 0.6 mg 2-CP can be adsorbed to 5 mg of MOF. Plus, 2-CP loaded MIL-101 was first dried for 12 h (120 °C) to prepare for measurement. The drying process might evaporate the molecule even though theoretically, the temperature is lower than 2-CP boiling point (175 °C). Besides, it may also be assumed that the adsorbed quantity is scarcely available on the MOF surface (constitutes 12% of MOF amount) to be detected by the FTIR instrument. 2-CP loaded AC and fresh AC samples were not able to be measured as the instrument is not suitable to detect dark-coloured material. An Attenuated Total Reflection (ATR) tip made from Germanium must be used instead of diamond.

It does not suffice for us to conclude the type of adsorption occurs with the adsorbents whether through physical or chemical sorption. It is reported that presence of physisorbed 2-CP on the surface can be confirmed when an absorption

Table 1 – Results from N_2 adsorption and desorption experiments.

Sample	BET surface area ($m^2\ g^{-1}$)	Pore volume ($cm^3\ g^{-1}$)	Pore diameter (nm)
Pristine MIL-101	2710	2.15	3.17
MIL-101 after 3 days in pH = 1	2712	1.56	2.31
MIL-101 after 3 days in pH = 11	2098	1.18	2.24
MIL-101-NH_2	1983	1.25	2.52
AC	1179	0.81	2.73

band at 1338 cm^{-1} and 3570 cm^{-1} appear (Alderman and Dellinger, 2005). These bands correspond to 2-CP O—H bending and stretching, respectively. None of them is observed on the spectra. Besides, Van der Waals interaction between the MOF and 2-CP albeit weak, can actually lead to tight packing of 2-CP within the pores such that the vibrational motion of the adsorbed species is strongly hindered (Andini et al., 2006).

The characteristic signals for amino-functionalized MIL-101-NH_2 can be observed at 1165, 3378 and 3494 cm^{-1}. The last two vibrations happen due to the asymmetric and symmetric N—H stretching of the amino group whereas the lower end band is caused by C—N stretching vibration. All signals are in accordance to values reported in literature (Bernt et al., 2011; Tian et al., 2016).

3.4. TGA

Fig. 1 shows that sample mass of AC only decreased slightly throughout the measurement, remaining stable up to 700 °C before showing signs of decomposition. The relatively stagnant phase also indicates high AC hydrophobicity since not much removal of weakly adsorbed water is observed before 150 °C (Krahnstöver et al., 2016). Mass loss above 700 °C corresponds to the decomposition of functional groups and the result of partial gasification of the least thermally stable fragments contained in the carbon structure (Bazan et al., 2016). As for MOFs, generally, there are three distinct weight loss steps. The first step between 30 °C and 150 °C refers to the loss of moisture adsorbed from air and residual solvents used for washing (EtOH and DMF) from the large cages (Tian et al., 2016). Next, strongly adsorbed water molecules are removed from the middle sized cages from 150 °C to 370 °C. Above 370 °C, compounds such as −OH and other coordinated groups are eliminated simultaneously causing MIL-101 framework decomposition (Bernt et al., 2011; Hong et al., 2009; Jhung et al., 2007; Karikkethu Prabhakaran and Deschamps, 2015). The TGA profile also shows that MIL-101 is more hydrophobic than MIL-101-NH_2 as the latter experienced greater weight loss (<150 °C). Details about respective weight loss in the three stages can be found in Table S1 in SI. TGA is deemed to be more sensitive in the determination of loss bound water molecules from the MOFs compared to using water contact angle which may be influenced by surrounding humidity and loose sample packing despite being pressed.

3.5. Adsorption equilibrium

Various equilibrium isotherm models are available to interpret adsorption mechanism, surface properties and adsorbent's affinity (Foo and Hameed, 2010). Referring to previous work on adsorption of phenolic compounds on AC (Aksu and Yener, 2001; Aktaş and Çeçen, 2007; Fierro et al., 2008; Hamdaoui and Naffrechoux, 2007; Özkaya, 2006) and MIL-101 (Liu et al., 2014), the equilibrium data will also be analysed using Langmuir and Freundlich isotherm models.

Table 2 – Calculated parameters from Langmuir isotherm model.

Adsorbent	q_m ($mg\ g^{-1}$)	b ($L\ mg^{-1}$)	R^2
MIL-101	121	0.03	0.9942
MIL-101-NH_2	84	−0.04	0.9764
AC	345	0.74	0.9990

3.5.1. Langmuir isotherm model

The Langmuir adsorption isotherm model is formed based on several assumptions including monolayer adsorption or localized adsorption. This means only one molecule can occupy a fixed number of vacant adsorption sites. Once the sites are fully occupied, no further adsorption can happen. Graphically, a plateau will be observed as the adsorbent reaches an equilibrium saturation point. Apart from that, all adsorption sites are considered to have similar sorption activation energy (each site has equal affinity for the adsorbate), adsorbed molecules do not have any interaction between each other and no transmigration of adsorbate in the plane of the surface (Arasteh et al., 2010; Fierro et al., 2008; Foo and Hameed, 2010; Langmuir, 1916). The mathematical expression of the model can be found in Table 3 while the calculations are presented in Table S2 of SI.

Apart from that, another dimensionless constant known as separation factor (R_L) can be used to determine the adsorption nature. Lower R_L value indicates a more favourable adsorption. It may sometimes be unfavourable ($R_L > 1$), linear ($R_L = 1$), favourable ($0 < R_L < 1$) or irreversible ($R_L = 0$) (Weber and Chakravorti, 1974). K_L stands as the Langmuir constant ($L\ mg^{-1}$) and C_o refers to the adsorbate initial concentration ($mg\ L^{-1}$). A brief comparison between the Langmuir constant values in Table 2 suggests the existence of strong interaction between AC and the solute.

$$R_L = \frac{1}{1 + K_L C_0}$$

Calculated R_L values are all between 0 and 1 (Table S3 of SI) signifying a favourable adsorption except for MIL-101-NH_2 giving negative values. Initial conclusion was that MIL-101-NH_2 does not follow Langmuir assumptions meaning it will not reach a certain limit with the increase in concentration. On another note, this might surmise a multilayer adsorption which can be fitted with a Freundlich isotherm model.

3.5.2. Freundlich isotherm model

Freundlich isotherm is widely used to describe non-ideal, reversible and multilayer adsorption over heterogeneous surface as opposed to the monolayer theory postulated by Langmuir (Freundlich, 1906). The equation can be seen in Table 3. Data fitting for MIL-101-NH_2 using Freundlich model led to really low regression coefficient value ($R^2 = 0.342$) compared to using Langmuir's. This is because minimal divergence seen in higher solute concentration may slightly alter the model linearity. Our conviction therefore leans more towards Langmuir isotherm if the data irregularity is ruled out.

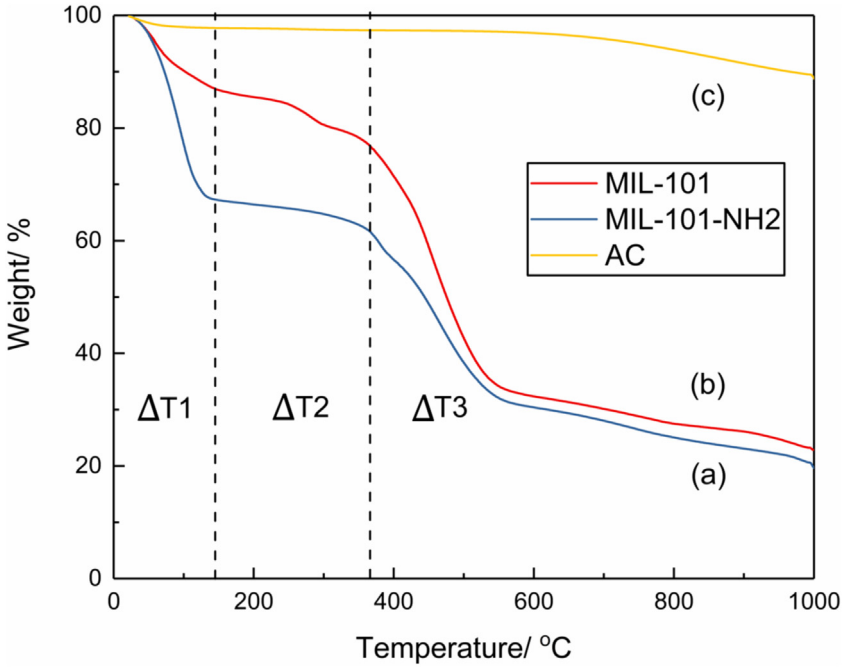

Fig. 1 – Weight loss profile of (a) MIL-101-NH_2, (b) MIL-101 and (c) AC when heated from 20 to 1000 °C.

Table 3 – Details of adsorption isotherm models.

Isotherm	Nonlinear form	Linear form	Plot	Reference
Langmuir	$q_e = \frac{q_m b C_e}{1+bC_e}$	$\frac{C_e}{q_e} = \frac{1}{q_m b} + \frac{C_e}{q_m}$	$\frac{C_e}{q_e}$ vs C_e	(Langmuir, 1916)
Freundlich	$q_e = K_F C_e^{\frac{1}{n}}$	$ln_{q_e} = ln_{K_F} + \frac{1}{n} ln_{C_e}$	ln_{q_e} vs ln_{C_e}	(Freundlich, 1906)

Where q_e is the amount of 2-CP adsorbed per unit mass of adsorbent (mg g^{-1}), b is a Langmuir constant related to free energy of adsorption (shares the same definition with aforementioned K_L) and C_e is residual concentration of adsorbate at equilibrium (mg L^{-1}), K_F is the Freundlich constant related to the adsorption capacity (mg g^{-1}.(mg L^{-1})^n) and 1/n is a parameter ranging from 0 to 1 which represents adsorption intensity or surface heterogeneity with the surface becoming more heterogeneous as it approaches 0 (Haghseresht and Lu, 1998).

3.6. *Batch adsorption studies*

Batch adsorption isotherm plots of 2-CP uptake by MIL-101 and MIL-101-NH_2 as observed in Fig. 2 are of L-type isotherm. In comparison to AC, it presents the characteristic of a H-class isotherm as there is a steep uptake at very low concentrations possibly due to the extremely strong adsorption (Dąbrowski et al., 2005; Hinz, 2001). Calculated maximum Langmuir adsorption capacity (q_m) are 345, 121 and 84 mg g^{-1} respectively for AC, MIL-101 and MIL-101-NH_2. The highest Langmuir adsorption capacity shown by AC agrees well with the literature (Aksu and Yener, 2001; Aktaş and Çeçen, 2007; Fierro et al., 2008; Hamdaoui and Naffrechoux, 2007; Özkaya, 2006) despite having the lowest surface area amongst all studied adsorbents.

Liquid-phase adsorption of guest molecules over MOFs can occur via several mechanisms including (1) electrostatic interaction, (2) acid-base interaction, (3) hydrogen bonding, (4) influence of framework metal, (5) π–π stacking/interaction and (6) hydrophobic interaction (Hasan and Jhung, 2015). Results from the experiments shown later are meant to illustrate how some of these factors contribute to the adsorption disparity. Both rate and magnitude of adsorption are dependent on many factors namely adsorbate molecular structure, solubility, ionization, reaction temperature and presence of multiple solutes (Perrich, 2018).

Looking at the 2-CP molecular structure and the excellent adsorption capacity shown by AC, it is deduced to be mainly driven by the dispersion interactions between π -electrons on the aromatic ring of 2-CP (Hamdaoui and Naffrechoux, 2007) and those aromatic sheets of the AC (Gorner et al., 2002). Similarly, on MOFs, the π - π stacking between the carboxyl group on the organic ligand network (Hu et al., 2013) and the phenyl ring of 2-CP can contribute to the adsorption too but neither of these MOFs shows significant 2-CP uptake. Given the totality of AC structure which is made up from randomly orientated aromatic rings in comparison to only a portion from the MOF ligand section, it may imply the existence of a stronger interaction than π - π stacking for the MOFs.

Next probable reason is given by the weak electron donor-acceptor complex relationship between 2-CP and the MOFs. Upon termination of water molecules through vacuum drying, the unsaturated Cr (III) Lewis acid sites on MIL-101 serve as electron acceptor (Huang et al., 2011) whereas the –chloro (Cl) substituent on 2-CP is an electron withdrawing group (EWG) (Jung et al., 2001). Thermal activation of AC usually leads to establishment of basic oxygen groups on the surface (Aktaş and Çeçen, 2007). This region, rich in electrons acts as donors (Okolo et al., 2000) and subsequently reduces the π -electrons of phenols while reinforcing the affinity to π -electrons on AC. Intuitively, this explains why existence of EWGs like –Cl and NO_2 on phenolic compounds favoured adsorption onto AC much more in contrast to attachment of electron donating groups (EDGs) like $-CH_3$ and $-CH_2CH_3$ (Lu and Sorial, 2007).

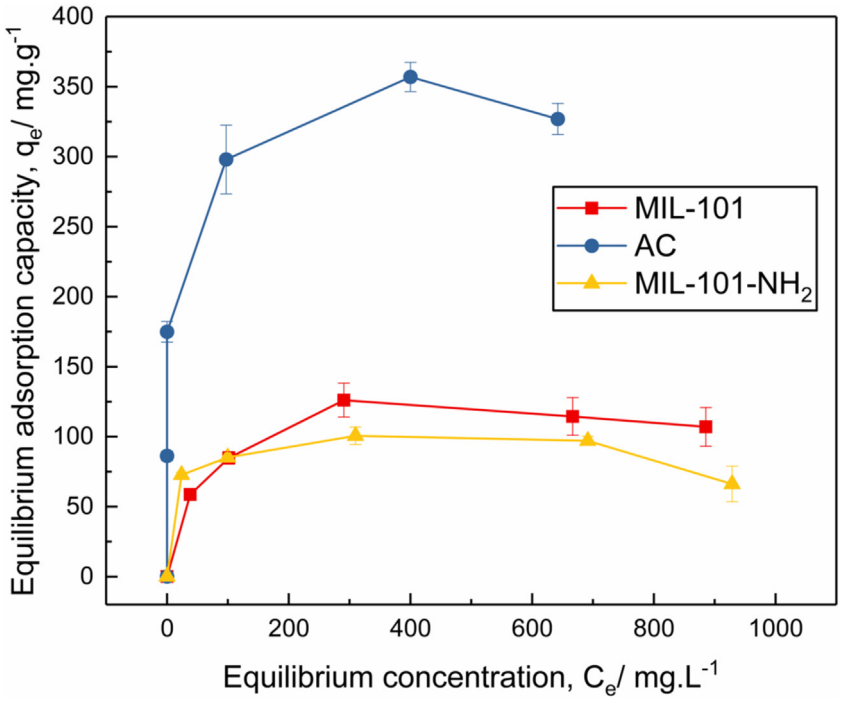

Fig. 2 – Plot of 2-CP uptake capacity at different solute concentration after 24 h adsorption.

Adsorption of organic molecules often involves a complex balance between non-electrostatic (dispersion and hydrophobicity) and electrostatic interactions. Hydrophobic interaction or specifically termed as hydrophobic bonding describes the unusual strong attraction between hydrophobic molecules and hydrophobic surfaces (Moreno-Castilla, 2004). AC demonstrated good 2-CP uptake possibly due to the low log K_{ow} value of 2-CP (2.15) which enabled strong hydrophobic-hydrophobic interactions (Chuang et al., 2008).

The selection of post-synthetically modified MIL-101-NH_2 used in this study was done to investigate the effect of adding –NH_2 moiety in relation to its adsorption performance compared to the pristine MIL-101. A similar MOF was used to remove hazardous pollutants like naproxen and clofibric acid. Their results demonstrated higher adsorption capacities on ED-MIL-101 (ethylene diamine) compared to pristine MIL-101 and AMSA-MIL-101 (aminomethanesulfonic acid) (Hasan et al., 2013). Functionalization of MIL-101 with ED made the MOF more basic with the addition of –NH_2 group. Interaction with the acidic –COOH group on the pollutants led to a stronger acid-base link between them. In this context, acid-base interaction is speculated to be less influential in the whole adsorption mechanism for MIL-101-NH_2 because of the NH_2-NH_2 and NH_2–OH hydrogen bonding interactions occurring between the respective moieties (Serra-Crespo et al., 2011). On the other hand, it is more obvious to say the expected hypothesis is true for the case of AC from the interaction between its basic surface oxygen groups and the slightly acidic 2-CP (Okolo et al., 2000).

Apart from that, the –NH_2 functionalization strategy also aims to bring forward the establishment of H-bonding with 2-CP. As expected, after modification, surface area of MIL-101-NH_2 decreased slightly compared to pristine MIL-101. The addition of –NH2 group occupied some space in the pores thus, reducing pore volume from 2.2 $cm^3.g^{-1}$ to 1.3 $cm^3.g^{-1}$. Among MOFs, data for batch adsorption isotherm proves that higher surface area is key as it provides more vacant adsorption sites. The competition between surface area and extrinsically introduced H-bond attractor does not seem as prevalent in this case. It can be the lone pair of NH_2-H_2BDC having higher possibility of forming H-bond with the surrounding water molecules thus, interfering effective 2-CP adsorption (Gao et al., 2013).

MIL-101-NH_2 derivative modified from MIL-101 has become more hydrophilic upon –NH_2 functionalization. MIL-101 is a widely acknowledged water stable MOF. Previous studies for MIL-101 have proven large water uptake capacity at a moderate humidity (1.0–1.4 g $H_2O.g^{-1}$ MOF at P/P_0 = 0.9). The hydrophilicity of MIL-101 is largely contributed by the influence of –COOH group in the BDC linker (Ko et al., 2015). Introducing hydrophilic groups like -NH_2 and -SO_3H promotes a more hydrophilic condition inside the pore; resulting to higher affinity of water molecules towards the pores (Akiyama et al., 2012). Such a hydrophilic MOF, when exposed to air or moisture, is likely to form surface barriers which will impede mass transfer rates in and out of the pores (Heinke et al., 2014). When molecular oxygen is present in the test environment (oxic condition), phenols are reported to undergo oligomerization. Consequently, the oligomerized phenols develop irreversible bond to the carbon surface and consolidates the high 2-CP uptake by AC (Lu and Sorial, 2007).

Results from another adsorption kinetic of 2-CP on solid catalyst, TiO_2 also demonstrated the existence of competitive adsorption between solvent (water in their case) and the pollutant at the same sites (Rideh et al., 1999). Presumably, MIL-101 hydrophilicity (Fig. S12 in SI) seems to be the biggest deterrent for efficient 2-CP adsorption unlike hydrophobic AC which can repel surrounding water molecules and preferentially adsorb the pollutant (Bhadra et al., 2015; Li et al., 2002).

3.7. *Kinetics*

The trend shown in Fig. 3 indicates quick adsorption of 2-CP into the pores of both adsorbents. To explain the adsorption process, it is important to match the pore size of adsorbent with the size of the adsorbate molecule (Jung et al., 2001). From

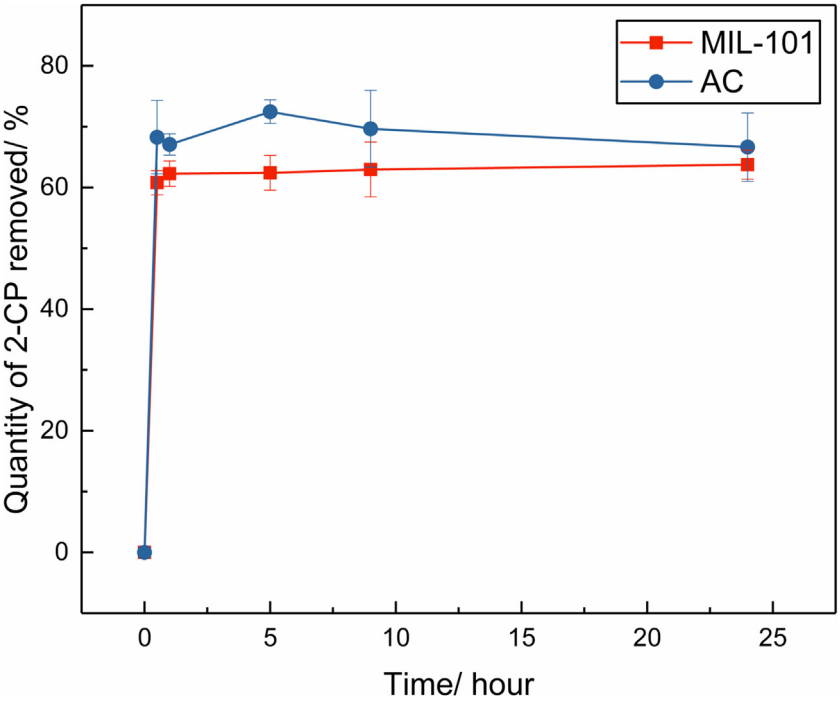

Fig. 3 – Amount of adsorbed 2-CP at specific time intervals.

the BET surface area analysis, MIL-101 has the highest pore diameter (32 Å) while AC has the lowest pore diameter (27 Å). Meanwhile, computational 2-CP molecular diameter (5.6 Å) is approximately between five and six times smaller than the available pore spaces. The ratio (adsorbent pore diameter to 2-CP molecular diameter) although not extensively large can affect diffusion of 2-CP in and out of the inner pores. The effect is more pronounced when reaction is taking place under rapid stirring mode especially with the time lag in between the filtration. Apart from that, given the pore size of syringe filter (0.22 μm) that was used, there may be some possibility of the adsorbents passing through the filter according to our particle size analysis (Table S4 of SI). So, adsorption may still take place even after stirring ceases. Nevertheless, both adsorbents reached an equilibrium state within the first hour. As the initial adsorption rate was very rapid, starting with a higher solute concentration will allow more time for the molecules to diffuse into the pores but batch-style exposure experiments were utilised in this study. Packing the sorbents either into columns or used as filters can render them suitable for commercial purification processes as well as the possibility of evaluating their kinetic difference.

From our batch adsorption studies, analysis was continued only with MIL-101 and AC as each adsorbent demonstrated contradicting adsorption performance with respect to their surface areas. Since MIL-101-NH_2 does not yield high 2-CP uptake, it is not further studied from this point onwards. Sorption experimental data were fitted with a pseudo second order (PSO) kinetic model (Liu et al., 2014) to elucidate the dynamics of adsorption as well as the factors affecting the rate. Results show that regression of non-linear method may be a better option to obtain the desired parameters (Ho, 2006a; Kumar, 2006) but due to lack of consistency in the data, the linear form was used in lieu. The observed regression coefficients (R^2) for the linear plots of t/q_t versus t are all greater than 0.999 (Fig. S8 and S9 in SI). This suggests that the rate-limiting step for the sorption system is chemical sorption. It is a strong interaction involving sharing of valence forces or exchange of electrons between sorbent and sorbate (Ho, 2006b). However, calculation could only be done to obtain kinetic rate constant (k_2) for MIL-101 as it is practically impossible to calculate k_2 for AC because of the negative intercept.

As previously mentioned, variations observed in the experimental data are severely limiting proper calculations to be made. Under these circumstances, the calculated values cannot be claimed to reflect the whole adsorption system. Related equations are shown in Table 4.

Where k_2 is the PSO kinetic rate constant (g.(mg.min)$^{-1}$), q_e is the equilibrium amount of solute adsorbed at equilibrium (mg.g^{-1}), t is the time, q_t is the adsorption capacity at a specific time.

3.8. *pH and zeta potential influence*

Adsorption experiments were conducted using a solute concentration of 500 ppm with a pH range from 1 to 13. As illustrated in Fig. 4, irrespective of the adsorbent, there was no significant influence of solution pH from pH 1 to 6 on the extraction of 2-CP. Performance-wise, AC once again surpassed the adsorption capacity of MIL-101 within that acidic pH range. This is in resonance with the aforementioned dispersive mechanisms; stronger acid-base interaction, higher hydrophobicity, electron donor-acceptor complexes and occurrence of $\pi - \pi$ stacking. Hydrophilicity of MIL-101 causes competition between 2-CP and water molecules. Since water can potentially form hydrogen bonds with the sites on MIL-101, access to remaining sites is blocked which may explain the reason for its superficial adsorption performance.

Phenols and their chlorinated forms are representatives of ionizable organic compounds (IOCs) (Kim et al., 2005). This means variation of solution pH can affect 2-CP speciation as well as surface charges on the adsorbents. 2-CP has a dissociation constant (pK_a) value of 8.56. If solution pH > 8.56, the dominating species is the anionic chlorophenolate. Conversely, when pH < 8.56, more molecular 2-CP will exist (Chuang et al., 2008). Increase in pH simultaneously increases

Table 4 – Mathematical expressions for pseudo second order kinetic model.

Type	Non-linear form	Linear form	Plot	Parameters
Pseudo second order	$q_t = \frac{k_2 q_e^2 t}{1+k_2 q_e t}$	$\frac{t}{q_t} = \frac{1}{k_2 q_e^2} + \frac{t}{q_e}$	$\frac{t}{q_t}$ vs. t	$q_e = \frac{1}{slope}$, $k_2 = \frac{slope^2}{intercept}$

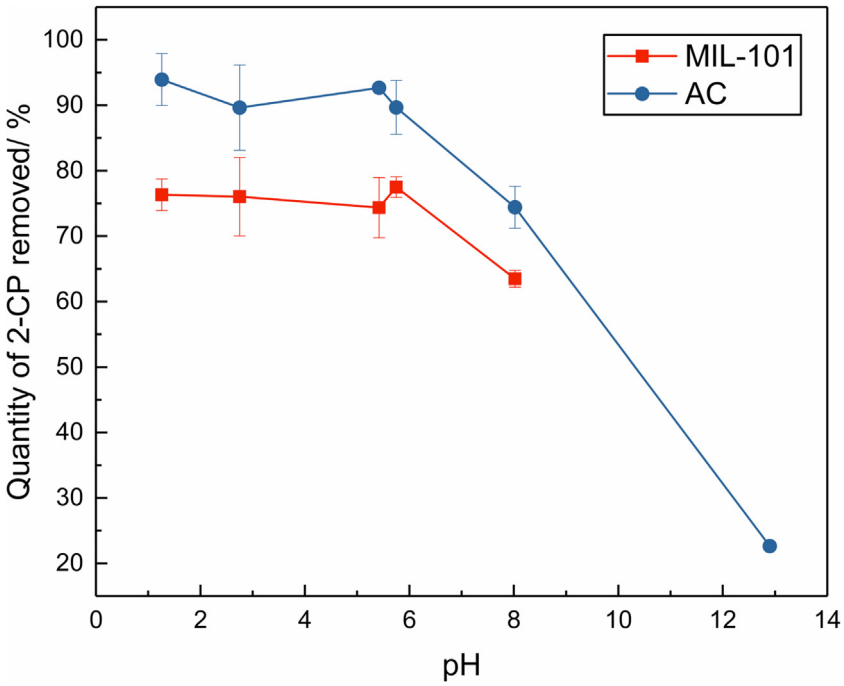

Fig. 4 – Influence of solution pH (1–13) to 2-CP uptake.

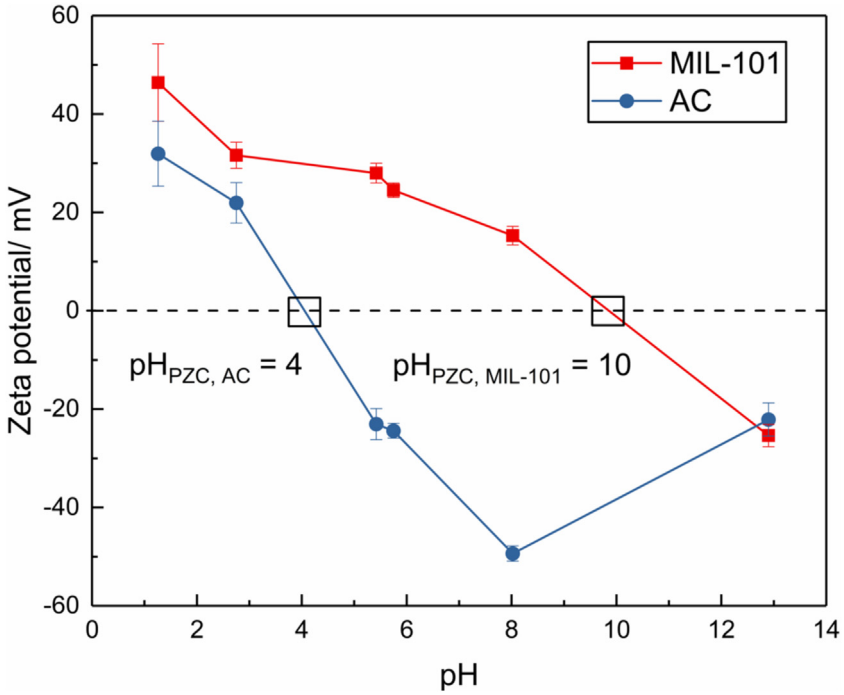

Fig. 5 – Zeta potential distribution for MIL-101 and AC across a pH range from 1 to 13. pH_{PZC} values for MIL-101 and AC are 10 and 4 respectively.

number of negatively charged sites on AC (Namasivayam and Kavitha, 2003) as can be observed in Fig. 5, especially after passing the point of zero charge (PZC) at pH = 4.

The accompanying drop of 2-CP uptake by both adsorbents beyond pH 6 may be explained by the presence of stronger electrostatic interaction. At pH 8, close to the pK_a of 2-CP, both molecular and anionic 2-CP species co-exist with similar proportions. Factors governing adsorption of both species are now competing with each other. At pH 13, the solution is almost dominated by chlorophenolate ions. Consequently, the electrostatic repulsion between the negatively charged adsorbent surfaces and the chlorophenolate species greatly reduced the adsorption capacity. Even though AC adsorption capacity is very low at high pH, some 2-CP can still be adsorbed.

The result can be ascribed to the presence of silica on the AC surface which bears surface hydroxyl sites of which 2-CP can chemisorb (Alderman and Dellinger, 2005; Namasivayam and Kavitha, 2003). Furthermore, the dissociated 2-CP is more soluble in basic aqueous solution; so, hydrogen bonds that are formed between water and chlorophenolate anions are stronger. As a result, it is difficult to break the bonds to permit 2-CP adsorption from the bulk phase (Villacañas et al., 2006).

In contrast to AC, MIL-101 carries higher positive charge and is more stable before its PZC (pH = 10) as can be seen in Fig. 5. Effect of surface charge destabilization after pH_{PZC} on its 2-CP removal performance cannot be observed in MIL-101 as dissolution happened in an extremely basic condition (pH = 13) forming a green-coloured suspension. Even after multiple filtrations, MIL-101 particles could not be segregated from the 2-CP solution. UV–vis measurement for this point is therefore inaccurate and opted out from the plot.

3.9. *Regeneration*

To demonstrate reusability of MOFs, 2-CP loaded MIL-101 was regenerated using a domestic solvent, ethanol (EtOH). Solvent exchange method utilizes readily available reagents, fast, and easy to handle which is why it is a cost-effective process compared to other techniques (Omorogie et al., 2016). The result shown in Fig. S10 of SI is however not conclusive as it is likely that the initial solute concentration is too low (100 ppm) against the maximum equilibrium adsorption capacity of MIL-101 (121 $mg.g^{-1}$). It needs to be optimized by starting with a higher concentration. For this case, the adsorption capacity increased almost doubled from its previous value. It was difficult to recover MIL-101 after centrifugation because of the small particle size. Mass loss is inevitable in this sense. Yet, it can be alluded to several reasons as to why even with lower mass of adsorbent, residual 2-CP is almost zero. What might happen when EtOH was used to wash the 2-CP loaded MOF is actually the phenomenon of pore clearing. Suppose if the washing frequency increases, it may lead to higher adsorption capacity until it reaches a certain threshold. Contradictory to MIL-101, after repeated ethanol washing, AC adsorption capacity appears to have slightly reduced possibly due to EtOH molecules occupying the pores. Overnight drying under vacuum condition at 120 °C may be insufficient to eliminate guest molecules from the pores of the samples. From the regeneration result, it is safe to assume that MIL-101 may perform better than AC for removal of 2-CP if more thorough washing and drying method after synthesis is performed to ensure all solvent molecules are removed. However, in reality, surrounding humidity cannot be easily isolated, hence, there must be a more pragmatic approach to curb this issue and make use of the MOF's high surface area. While knowing the promising performance shown by regenerated MIL-101, the material hitherto still has limitations to reach industrial or large scale production; lagging behind some other MOFs (Evans et al., 2019; Kirchon et al., 2018; Vo et al., 2019). Thus, promulgation of more studies heading to such direction can help find its future and practical prospects alongside with already commercialized MOFs and conventional adsorbents.

4. Conclusions

In summary, sorption performance of 2-CP on a commercial AC appears to be better compared to when using MOFs. Maximum equilibrium 2-CP uptake by AC is highest (345 $mg.g^{-1}$), followed by MIL-101 (121 $mg.g^{-1}$) and MIL-101-NH_2 (84 $mg.g^{-1}$) although the decreasing order of material surface area is MIL-101 > MIL-101-NH_2 > AC. High external surface area by MOFs therefore does not guarantee higher uptake but it depends on the inherent adsorbate-adsorbent interaction. Excellent 2-CP removal by AC is governed by its hydrophobicity and abundance of basic oxygen surface sites. 2-CP can only be effectively removed by MIL-101 after repeated ethanol washing. Finally, to utilize the high surface area of MOFs, one must prioritize a hydrophobic-type adsorbent to minimize the risk of competitive pollutant adsorption with water or moisture.

Conflict of interests

The authors declare that they have no known competing financial interests or personal relationships that could have appeared to influence the work reported in this paper.

Acknowledgements

Mohd Azmi, L. H. would like to extend his gratitude to Yayasan Khazanah for funding his PhD studies. The authors also acknowledge use of characterization facilities within the Harvey Flower Electron Microscopy Suite, Department of Materials, Imperial College London.

Appendix A. Supplementary data

Supplementary material related to this article can be found, in the online version, at doi:https://doi.org/10.1016/j.cherd.2020.03.017. The raw data presented in the figures can be accessed from the open repository: https://doi.org/10.5281/zenodo.3545985

References

Akiyama, G., Matsuda, R., Sato, H., Hori, A., Takata, M., Kitagawa, S., 2012. Effect of functional groups in MIL-101 on water sorption behavior. Microporous Mesoporous Mater. 157, 89–93, http://dx.doi.org/10.1016/j.micromeso.2012.01.015.

Aksu, Z., Yener, J., 2001. A comparative adsorption/biosorption study of mono-chlorinated phenols onto various sorbents. Waste Manag. 21, 695–702.

Aktaş, Ö., Çeçen, F., 2007. Adsorption, desorption and bioregeneration in the treatment of 2-chlorophenol with activated carbon. J. Hazard. Mater. 141, 769–777.

Alderman, S.L., Dellinger, B., 2005. FTIR investigation of 2-chlorophenol chemisorption on a silica surface from 200 to 500°C. J. Phys. Chem. A 109, 7725–7731.

Andini, S., Cioffi, R., Montagnaro, F., Pisciotta, F., Santoro, L., 2006. Simultaneous adsorption of chlorophenol and heavy metal ions on organophilic bentonite. Appl. Clay Sci. 31, 126–133.

Arasteh, R., Masoumi, M., Rashidi, A.M., Moradi, L., Samimi, V., Mostafavi, S.T., 2010. Adsorption of 2-nitrophenol by multi-wall carbon nanotubes from aqueous solutions. Appl. Surf. Sci. 256, 4447–4455.

Bazan, A., Nowicki, P., Półrolniczak, P., Pietrzak, R., 2016. Thermal analysis of activated carbon obtained from residue after supercritical extraction of hops. J. Therm. Anal. Calorim. 125, 1199–1204.

Bernt, S., Guillerm, V., Serre, C., Stock, N., 2011. Direct covalent post-synthetic chemical modification of Cr-MIL-101 using nitrating acid. Chem. Commun. (Camb.) 47, 2838–2840, http://dx.doi.org/10.1039/c0cc04526h.

Bhadra, B.N., Cho, K.H., Khan, N.A., Hong, D.Y., Jhung, S.H., 2015. Liquid-phase adsorption of aromatics over a metal-organic

framework and activated carbon: effects of hydrophobicity/hydrophilicity of adsorbents and solvent polarity. J. Phys. Chem. C 119, 26620–26627, http://dx.doi.org/10.1021/acs.jpcc.5b09298.
Burgher, F., Mathieu, L., Lati, E., Gasser, P., Peno-Mazzarino, L., Blomet, J., Hall, A.H., Maibach, H.I., 2011. Experimental 70% hydrofluoric acid burns: histological observations in an established human skin explants ex vivo model. Cutan. Ocul. Toxicol. 30, 100–107.
Chemviron Carbon, 2013. Filtrasorb ® 400 Agglomerated Coal Based Granular Activated Carbon.
Chuang, Y.H., Tzou, Y.M., Wang, M.K., Liu, C.H., Chiang, P.N., 2008. Removal of 2-chlorophenol from aqueous solution by Mg/Al layered double hydroxide (LDH) and modified LDH. Ind. Eng. Chem. Res. 47, 3813–3819.
Czaplicka, M., 2004. Sources and transformations of chlorophenols in the natural environment. Sci. Total Environ. 322, 21–39.
Dąbrowski, A., Podkościelny, P., Hubicki, Z., Barczak, M., 2005. Adsorption of phenolic compounds by activated carbon—a critical review. Chemosphere 58, 1049–1070.
Dobaradaran, S., Nodehi, R.N., Yaghmaeian, K., Jaafari, J., Niari, M.H., Bharti, A.K., Agarwal, S., Gupta, V.K., Azari, A., Shariatifar, N., 2018. Catalytic decomposition of 2-chlorophenol using an ultrasonic-assisted Fe3O4–TiO2@ MWCNT system: influence factors, pathway and mechanism study. J. Colloid Interface Sci. 512, 172–189.
European Communities, 2001. Decision No. 2455/2001/EC of the European Parliament and of the Council of 20 November 2001 establishing the list of priority substances in the field of water policy and amending Directive 2000/60/EC. Off. J. Eur. Commun. 44, 1–5.
Evans, J.D., Garai, B., Reinsch, H., Li, W., Dissegna, S., Bon, V., Senkovska, I., Fischer, R.A., Kaskel, S., Janiak, C., 2019. Metal–organic frameworks in Germany: from synthesis to function. Coord. Chem. Rev. 380, 378–418.
Fierro, V., Torné-Fernández, V., Montané, D., Celzard, A., 2008. Adsorption of phenol onto activated carbons having different textural and surface properties. Microporous Mesoporous Mater. 111, 276–284.
Foo, K.Y., Hameed, B.H., 2010. Insights into the modeling of adsorption isotherm systems. Chem. Eng. J. 156, 2–10.
Freundlich, H.M.F., 1906. Over the adsorption in solution. J. Phys. Chem. 57, 1100–1107.
Gan, L., Li, B., Guo, M., Weng, X., Wang, T., Chen, Z., 2018. Mechanism for removing 2, 4-dichlorophenol via adsorption and Fenton-like oxidation using iron-based nanoparticles. Chemosphere 206, 168–174.
Gao, L., Li, C.-Y.V., Yung, H., Chan, K.-Y., 2013. A functionalized MIL-101 (Cr) metal–organic framework for enhanced hydrogen release from ammonia borane at low temperature. Chem. Commun. (Camb.) 49, 10629–10631.
Gorner, T., Villiéras, F., Polakovič, M., De Donato, P., Garnier, C., Paiva-Cabral, M., Bersillon, J.L., 2002. Inverse liquid chromatography investigation of adsorption on heterogeneous solid surfaces: phenylalanine on activated carbon. Langmuir 18, 8546–8552, http://dx.doi.org/10.1021/la0261139.
Gu, Z.-Y., Yang, C.-X., Chang, N., Yan, X.-P., 2012. Metal–organic frameworks for analytical chemistry: from sample collection to chromatographic separation. Acc. Chem. Res. 45, 734–745, http://dx.doi.org/10.1021/ar2002599.
Hadjltaief, H.B., Sdiri, A., Ltaief, W., Da Costa, P., Galvez, M.E., Zina, M.Ben, 2018. Efficient removal of cadmium and 2-chlorophenol in aqueous systems by natural clay: adsorption and photo-Fenton degradation processes. Comptes Rendus Chim. 21, 253–262.
Haghseresht, F., Lu, G.Q., 1998. Adsorption characteristics of phenolic compounds onto coal-reject-derived adsorbents. Energy Fuels 12, 1100–1107.
Hamdaoui, O., Naffrechoux, E., 2007. Modeling of adsorption isotherms of phenol and chlorophenols onto granular activated carbon: Part I. Two-parameter models and equations allowing determination of thermodynamic parameters. J. Hazard. Mater. 147, 381–394.
Han, S., Lah, M.S., 2015. Simple and efficient regeneration of MOF-5 and HKUST-1 via acid–base treatment. Cryst. Growth Des. 15, 5568–5572.
Hasan, Z., Jhung, S.H., 2015. Removal of hazardous organics from water using metal-organic frameworks (MOFs): plausible mechanisms for selective adsorptions. J. Hazard. Mater. 283, 329–339, http://dx.doi.org/10.1016/j.jhazmat.2014.09.046.
Hasan, Z., Jeon, J., Jhung, S.H., 2012. Adsorptive removal of naproxen and clofibric acid from water using metal-organic frameworks. J. Hazard. Mater. 209–210, 151–157, http://dx.doi.org/10.1016/j.jhazmat.2012.01.005.
Hasan, Z., Choi, E.J., Jhung, S.H., 2013. Adsorption of naproxen and clofibric acid over a metal–organic framework MIL-101 functionalized with acidic and basic groups. Chem. Eng. J. 219, 537–544, http://dx.doi.org/10.1016/j.cej.2013.01.002.
Heinke, L., Gu, Z., Wöll, C., 2014. The surface barrier phenomenon at the loading of metal-organic frameworks. Nat. Commun. 5, 4562.
Hinz, C., 2001. Description of sorption data with isotherm equations. Geoderma 99, 225–243.
Ho, Y.S., 2006a. Second-order kinetic model for the sorption of cadmium onto tree fern: a comparison of linear and non-linear methods. Water Res. 40, 119–125.
Ho, Y.S., 2006b. Review of second-order models for adsorption systems. J. Hazard. Mater. 136, 681–689.
Hong, D.Y., Hwang, Y.K., Serre, C., Férey, G., Chang, J.S., 2009. Porous chromium terephthalate MIL-101 with coordinatively unsaturated sites: Surface functionalization, encapsulation, sorption and catalysis. Adv. Funct. Mater. 19, 1537–1552, http://dx.doi.org/10.1002/adfm.200801130.
Hu, Y., Song, C., Liao, J., Huang, Z., Li, G., 2013. Water stable metal-organic framework packed microcolumn for online sorptive extraction and direct analysis of naproxen and its metabolite from urine sample. J. Chromatogr. A 1294, 17–24, http://dx.doi.org/10.1016/j.chroma.2013.04.034.
Huang, C.Y., Song, M., Gu, Z.Y., Wang, H.F., Yan, X.P., 2011. Probing the adsorption characteristic of metal-organic framework MIL-101 for volatile organic compounds by quartz crystal microbalance. Environ. Sci. Technol. 45, 4490–4496, http://dx.doi.org/10.1021/es200256q.
Ismail, A.F., Khulbe, K.C., Matsuura, T., 2015. Gas Separation Membranes: Polymeric and Inorganic. Springer International Publishing.
Jang, H.M., Yoo, S., Choi, Y.-K., Park, S., Kan, E., 2018. Adsorption isotherm, kinetic modeling and mechanism of tetracycline on Pinus taeda-derived activated biochar. Bioresour. Technol. 259, 24–31.
Jhung, S.H., Lee, J.H., Yoon, J.W., Serre, C., Férey, G., Chang, J.S., 2007. Microwave synthesis of chromium terephthalate MIL-101 and its benzene sorption ability. Adv. Mater. 19, 121–124, http://dx.doi.org/10.1002/adma.200601604.
Jung, M.-W., Ahn, K.-H., Lee, Y., Kim, K.-P., Rhee, J.-S., Park, J.T., Paeng, K.-J., 2001. Adsorption characteristics of phenol and chlorophenols on granular activated carbons (GAC). Microchem. J. 70, 123–131.
Karikkethu Prabhakaran, P., Deschamps, J., 2015. Doping activated carbon incorporated composite MIL-101 using lithium: impact on hydrogen uptake. J. Mater. Chem. A 3 (13), 7014–7021, http://dx.doi.org/10.1039/c4ta07197b.
Khan, N.A., Jung, B.K., Hasan, Z., Jhung, S.H., 2015. Adsorption and removal of phthalic acid and diethyl phthalate from water with zeolitic imidazolate and metal-organic frameworks. J. Hazard. Mater. 282, 194–200, http://dx.doi.org/10.1016/j.jhazmat.2014.03.047.
Kim, J.-H., Shin, W.S., Kim, Y.-H., Choi, S.-J., Jo, W.-K., Song, D.-I., 2005. Sorption and desorption kinetics of chlorophenols in hexadecyltrimethyl ammonium-montmorillonites and their model analysis. Korean J. Chem. Eng. 22, 857–864.
Kirchon, A., Day, G.S., Fang, Y., Banerjee, S., Ozdemir, O.K., Zhou, H.C., 2018. Suspension processing of microporous

metal-organic frameworks: a scalable route to high-quality adsorbents. iScience 5, 30–37.
Ko, N., Choi, P.G., Hong, J., Yeo, M., Sung, S., Cordova, K.E., Park, H.J., Yang, J.K., Kim, J., 2015. Tailoring the water adsorption properties of MIL-101 metal–organic frameworks by partial functionalization. J. Mater. Chem. A 3 (5), 2057–2064, http://dx.doi.org/10.1039/C4TA04907A.
Kolpin, D.W., Furlong, E.T., Meyer, M.T., Thurman, E.M., Zaugg, S.D., Barber, L.B., Buxton, H.T., 2002. Pharmaceuticals, hormones, and other organic wastewater contaminants in US streams, 1999−2000: a national reconnaissance. Environ. Sci. Technol. 36, 1202–1211.
Krahnstöver, T., Plattner, J., Wintgens, T., 2016. Quantitative detection of powdered activated carbon in wastewater treatment plant effluent by thermogravimetric analysis (TGA). Water Res. 101, 510–518.
Kumar, K.V., 2006. Linear and non-linear regression analysis for the sorption kinetics of methylene blue onto activated carbon. J. Hazard. Mater. 137, 1538–1544.
Langmuir, I., 1916. The constitution and fundamental properties of solids and liquids. Part I. Solids. J. Am. Chem. Soc. 38, 2221–2295.
Li, L., Quinlivan, P.A., Knappe, D.R.U., 2002. Effects of activated carbon surface chemistry and pore structure on the adsorption of organic contaminants from aqueous solution. Carbon 40, 2085–2100.
Li, J., Chen, Y., Wu, Q., Wu, J., Xu, Y., 2019. Synthesis of sea-urchin-like Fe 3 O 4/SnO 2 heterostructures and its application for environmental remediation by removal of p-chlorophenol. J. Mater. Sci. 54, 1341–1350.
Liang, J., Fang, X., Lin, Y., Wang, D., 2018. A new screened microbial consortium OEM2 for lignocellulosic biomass deconstruction and chlorophenols detoxification. J. Hazard. Mater. 347, 341–348.
Liu, B., Yang, F., Zou, Y., Peng, Y., 2014. Adsorption of phenol and p-nitrophenol from aqueous solutions on metal–organic frameworks: effect of hydrogen bonding. J. Chem. Eng. Data 59, 1476–1482.
Lu, Q., Sorial, G.A., 2007. The effect of functional groups on oligomerization of phenolics on activated carbon. J. Hazard. Mater. 148, 436–445.
Luo, Y., Su, Y., Lin, R., Shi, H., Wang, X., 2006. 2-Chlorophenol induced ROS generation in fish Carassius auratus based on the EPR method. Chemosphere 65, 1064–1073.
Martínez-Jardines, M., Martínez-Hernández, S., Texier, A.-C., Cuervo-López, F., 2018. 2-Chlorophenol consumption by cometabolism in nitrifying SBR reactors. Chemosphere 212, 41–49.
Moreno-Castilla, C., 2004. Adsorption of organic molecules from aqueous solutions on carbon materials. Carbon 42, 83–94.
Morlay, C., Pilshofer, M., Quivet, E., Faure, R., Joly, J., 2005. Adsorption Isotherms of an Imidazolinone Herbicide on Activated Carbon. Abstracts of Papers of the American Chemical Society, p. U851.
Moura, F.C.C., Rios, R.D.F., Galvão, B.R.L., 2018. Emerging contaminants removal by granular activated carbon obtained from residual Macauba biomass. Environ. Sci. Pollut. Res. 25, 26482–26492.
Namasivayam, C., Kavitha, D., 2003. Adsorptive removal of 2-chlorophenol by low-cost coir pith carbon. J. Hazard. Mater. 98, 257–274.
Okolo, B., Park, C., Keane, M.A., 2000. Interaction of phenol and chlorophenols with activated carbon and synthetic zeolites in aqueous media. J. Colloid Interface Sci. 226, 308–317.
Olaniran, A.O., Igbinosa, E.O., 2011. Chlorophenols and other related derivatives of environmental concern: properties, distribution and microbial degradation processes. Chemosphere 83, 1297–1306.
Omorogie, M.O., Babalola, J.O., Unuabonah, E.I., 2016. Regeneration strategies for spent solid matrices used in adsorption of organic pollutants from surface water: a critical review. Desalin. Water Treat. 57, 518–544.
Özkaya, B., 2006. Adsorption and desorption of phenol on activated carbon and a comparison of isotherm models. J. Hazard. Mater. 129, 158–163.
Perrich, J.R., 2018. Activated Carbon Adsorption For Wastewater Treatment. CRC Press.
Rallapalli, P., Raj, M.C., Senthilkumar, S., Somani, R.S., Bajaj, H.C., 2016. HF-free synthesis of MIL-101 (Cr) and its hydrogen adsorption studies. Environ. Prog. Sustain. Energy 35, 461–468.
Rideh, L., Wehrer, A., Ronze, D., Zoulalian, A., 1999. Modelling of the kinetic of 2-chlorophenol catalytic photooxidation. Catal. Today 48, 357–362.
Seo, P.W., Khan, N.A., Hasan, Z., Jhung, S.H., 2016. Adsorptive removal of artificial sweeteners from water using metal-organic frameworks functionalized with urea or melamine. ACS Appl. Mater. Interfaces 8, 29799–29807, http://dx.doi.org/10.1021/acsami.6b11115.
Serra-Crespo, P., Ramos-Fernandez, E.V., Gascon, J., Kapteijn, F., 2011. Synthesis and characterization of an amino functionalized MIL-101 (Al): separation and catalytic properties. Chem. Mater. 23, 2565–2572.
Shang, N.C., Yu, Y.H., Ma, H.W., Chang, C.H., Liou, M.L., 2006. Toxicity measurements in aqueous solution during ozonation of mono-chlorophenols. J. Environ. Manage. 78, 216–222.
Sharma, S., Mukhopadhyay, M., Murthy, Z.V.P., 2013. Treatment of chlorophenols from wastewaters by advanced oxidation processes. Sep. Purif. Rev. 42, 263–295.
Smolin, S.K., 2018. Self-regeneration of a fixed bed of biologically activated carbon during removal of 2-chlorophenol from water. J. Water Chem. Technol. 40, 258–264.
Sonnauer, A., Hoffmann, F., Fröba, M., Kienle, L., Duppel, V., Thommes, M., Serre, C., Férey, G., Stock, N., 2009. Giant pores in a chromium 2, 6-naphthalenedicarboxylate open-framework structure with MIL-101 topology. Angew. Chem. 121, 3849–3852.
Stockholm Convention Secretariat United Nations Environment, 2017. The 16 New POPs, Stockholm Convention on Persistent Organic Pollutants (POPs). UN Environment, pp. 1–25.
Sühnholz, S., Kopinke, F.D., Weiner, B., 2018. Hydrothermal treatment for regeneration of activated carbon loaded with organic micropollutants. Sci. Total Environ. 644, 854–861.
Sun, Z., Zhang, J., Yang, J., Li, J., Wang, J., Hu, X., 2018. Acclimation of 2-chlorophenol-biodegrading activated sludge and microbial community analysis. Water Environ. Res. 90, 2083–2089.
The United Kingdom Parliamentary Office of Science and Technology, 2018. Persistent Chemical Pollutants.
Tian, N., Jia, Q., Su, H., Zhi, Y., Ma, A., Wu, J., Shan, S., 2016. The synthesis of mesostructured NH2-MIL-101 (Cr) and kinetic and thermodynamic study in tetracycline aqueous solutions. J. Porous Mater. 23, 1269–1278.
United Nations World Water Assessment Programme, 2018. The United Nations World Water Development Report 2018: Nature-Based Solutions for Water, UN Water Report. UNESCO, Paris.
United States Environmental Protection Agency, 2014. Priority Pollutant List, Effluent Guidelines.
Van de Voorde, B., Bueken, B., Denayer, J., De Vos, D., 2014. Adsorptive separation on metal–organic frameworks in the liquid phase. Chem. Soc. Rev. 43, 5766–5788, http://dx.doi.org/10.1039/C4CS00006D.
Vashi, H., Iorhemen, O.T., Tay, J.H., 2018. Aerobic granulation: a recent development on the biological treatment of pulp and paper wastewater. Environ. Technol. Innov. 9, 265–274.
Villacañas, F., Pereira, M.F.R., Órfão, J.J.M., Figueiredo, J.L., 2006. Adsorption of simple aromatic compounds on activated carbons. J. Colloid Interface Sci. 293, 128–136.
Vo, T.K., Kim, J.H., Kwon, H.T., Kim, J., 2019. Cost-effective and eco-friendly synthesis of MIL-101 (Cr) from waste hexavalent chromium and its application for carbon monoxide separation. J. Ind. Eng. Chem. 80, 345–351.
Weber, T.W., Chakravorti, R.K., 1974. Pore and solid diffusion models for fixed-bed adsorbers. AIChE J. 20, 228–238.

World Health Organization, 2003. Chlorophenols in drinking-water. In: Guidelines for Drinking Water Quality., http://dx.doi.org/10.1016/j.kjms.2011.05.002, Geneva.
Zhang, J., Tian, B., Wang, L., Xing, M., Lei, J., 2018. Heterogeneous photo-fenton technology. Photocatalysis 100, 241–258.
Zhao, T., Jeremias, F., Boldog, I., Nguyen, B., Henninger, S.K., Janiak, C., 2015. High-yield, fluoride-free and large-scale synthesis of MIL-101(Cr). Dalton Trans. 44, 16791–16801, http://dx.doi.org/10.1039/C5DT02625C.
Zhao, T., Yang, L., Feng, P., Gruber, I., Janiak, C., Liu, Y., 2017. Facile synthesis of nano-sized MIL-101 (Cr) with the addition of acetic acid. Inorganica Chim. Acta 471, 440–445.